Catalysis of Stark-tuned interactions between ultracold Rydberg atoms

A. L. Win, W. D. Williams, T. J. Carroll, and C. I. Sukenik

Catalysis of Stark-tuned interactions between ultracold Rydberg atoms

A.L. Win,[1] W.D. Williams,[2] T.J. Carroll,[3] and C.I. Sukenik[1]

[1]*Department of Physics, Old Dominion University, Norfolk, VA 23529, USA*
[2]*Department of Physics, Smith College, Northampton, MA 01063, USA*
[3]*Department of Physics and Astronomy, Ursinus College, Collegeville, PA, 19426 USA*
(Dated: August 23, 2018)

We have experimentally investigated a catalysis effect in the resonant energy transfer between ultracold ^{85}Rb Rydberg atoms. We studied the time-dependence of the process: $34p + 34p \rightarrow 34s + 35s$ and observed an enhancement of $34s$ state population when $34d$ state atoms are added. We have also performed numerical model simulations, which are in qualitative agreement with experiment and indicate that the enhancement arises from a redistribution of p-state atoms due to the presence of the d-state atoms.

The dynamics that result from interactions between Rydberg atoms produced in dilute ultracold atomic vapors differ from Rydberg gases at room temperature [1]. At ultracold temperatures, Rydberg atoms move only a few percent of their interatomic spacing, $\sim 10~\mu$m, during the few microseconds over which they typically interact. These atoms, therefore, are essentially frozen in place and are accordingly referred to as a "frozen Rydberg gas" [2]. While the small motion can be important [3], even in the static approximation, dipole-dipole coupling can lead to changes in the atomic state through an energy transfer process. For example, two atoms initially in a p state may end up in an s state via a process of the form $np+np \rightarrow ns+(n+1)s$. This is most likely to occur if the energy defect between the initial atom pair and the final atom pair is zero. Although in general this is never the case, a small energy defect can be nulled and the process brought into resonance by placing the atoms in a static electric field. Such "Stark-tuning" yields what is known as a Förster resonance. Such resonances have been studied experimentally [4–11] and theoretically [12, 13]. Förster resonances have also been studied in microwave or other ac fields [14–22]. Additionally, the dynamics of an ensemble of Rydberg atoms can depend on binary interactions and many-body effects [23–35] as well as the multi-level structure of the atom [36]. The importance of many-body interactions induced by introducing additional Rydberg atoms (that were strongly coupled to one of the final states) to a Stark-tuned resonant energy transfer process between Rydberg atoms initially in different states was demonstrated in [37]. Central to understanding many of these energy transfer processes is realizing that in addition to the Förster resonances, there exists dipole-dipole interaction channels that are *always* resonant, independent of electric field, and that these give rise to many-body effects in the dynamics of the Förster resonance [38].

There has been significant interest in using Rydberg atoms to model the energy transport in diverse physical systems [39–43]. Recent theoretical work has studied the motion of individual excitations through such a system [44] and shown that interacting Rydberg atoms could be used as a quantum simulator for other many-body quantum systems [45]. Dipole-dipole mediated energy exchange has also been studied in simulation in lattices [46] and the effect of anisotropy has been simulated in amorphous samples [47]. The energy exchange in a Rydberg atom system has also been directly imaged in experiment, measuring the diffusion rate of Rydberg excitons [48] and observing energy exchange over a spatial gap [49].

In this paper, we report on our investigation of what we call a Förster resonance "catalysis" effect induced by the addition of Rydberg atoms that are coupled to the initial state atoms, but do not directly participate in the resonant energy transfer process. These atoms enable a spatially dependent control mechanism of the Förster resonance. Specifically, we have investigated the process $34p + 34p \rightarrow 34s + 35s$ by initially exciting a collection of $34p$ atoms and measuring the number that end up in the $34s$ state. We observe more efficient energy transport, increasing the population of $34s$ atoms, when a relatively smaller and denser overlapping volume of $34d$ Rydberg atoms is added to the atomic ensemble. While simply exciting additional $34p$ atoms would also increase the population of $34s$ atoms, this paper explores the dynamics of increasing the $34s$ population via the addition of a controllable channel to redistribute $34p$ population in the atomic sample. This new "knob" provides a mechanism to influence the temporal dynamics and control the spatial distribution of atomic populations via a tunable process that can either increase or decrease the rate of energy transfer.

With only $34p$ state atoms initially excited, the process under investigation has three interaction channels:

$$34p + 34p \rightarrow 34s + 35s, \tag{1a}$$

$$34p + 34s \rightarrow 34s + 34p, \tag{1b}$$

$$34p + 35s \rightarrow 35s + 34p, \tag{1c}$$

with the latter two channels always resonant. By intro-

ducing Rydberg atoms in the $34d$ state, another always resonant channel is added, namely,

$$34p + 34d \rightarrow 34d + 34p. \qquad (2)$$

This channel redistributes the $34p$ population, which results in an enhancement of the process in Eq. (1a) at early times in our experiment.

The experiment begins with ^{85}Rb atoms confined in a magneto-optical trap (MOT). Atoms are excited with pulsed lasers to Rydberg states, an electric field is applied to the atoms for a variable time and state-selective field ionization is used to readout the population of Rydberg levels. Excitation to the $34p$ Rydberg state is via a single photon transition from the $5s_{1/2}$ ground state with light at $\lambda \sim 298$ nm (~ 0.5 mJ/pulse; linewidth ~ 0.1 cm^{-1}), derived from a frequency doubled, pulsed dye laser (Continuum ND6000), pumped by a Nd:YAG laser. Excitation to the $34d$ state proceeds via a two-step process: $5s_{1/2} \rightarrow 5p_{3/2} \rightarrow 34d$ with $\lambda_1 \sim 780$ nm (~ 80 μJ/pulse) and $\lambda_2 \sim 481$ nm (~ 0.2 mJ/pulse; linewidth ~ 0.1 cm^{-1}) with light from two additional pulsed dye lasers that are both pumped by a second Nd:YAG laser. The 780 nm laser is a homebuilt, flowing dye laser and the 481 nm laser is a Quantel TDL60. All three lasers have a pulse width of ~ 5 ns and a repetition rate of 10 Hz. The Nd:YAG pump lasers are synchronized to each other. The 298 nm laser beam passes through a 200 mm quartz lens giving a (calculated) 40 μm beam waist that was translated so as to maximize $34p$ counts and likely fills the MOT. The 481 nm laser passed through a 250 mm quartz lens giving a (calculated) ~ 80 μm beam waist that pierced the MOT after being combined with the 780 nm laser on a dichroic beamsplitter. Adjustment of the 298 nm laser polarization enabled some control of magnetic substate selection of the $34p$ state. The flash-lamp synchronization output from one of the Nd:YAG lasers triggers a digital delay pulse generator that controls the subsequent timing of the experiment. Both Nd:YAG laser pulses arrive within 1 μs of each other. Just before these pulses arrive, the MOT lasers are extinguished. The MOT magnetic field gradient of ~ 10 Gauss/cm remains on throughout the entire experiment. Next, 100 ns after excitation, a low voltage pulse is applied to one of two transparent meshes that surround the MOT in order to Stark-tune the resonance. After a variable delay, a high voltage pulse with a rise-time of ~ 8 μs is applied to the mesh and time-resolved pulses from a channel electron multiplier (CEM) configured to detect ions are counted with a multichannel scaler after passing through a fast pre-amplifier.

The calculated Stark structure of the pair states of $34p_{3/2}$ atoms reveals the crossings of the energy levels with $34s_{1/2} + 35s_{1/2}$ at the fields for Förster resonances as shown in the inset to Fig.1(a). The pair states $34p_{3/2} + 34p_{3/2}$ and $34s_{1/2} + 35s_{1/2}$ are 572.5 MHz apart in energy at zero electric field [50]. Fig.1 shows – for
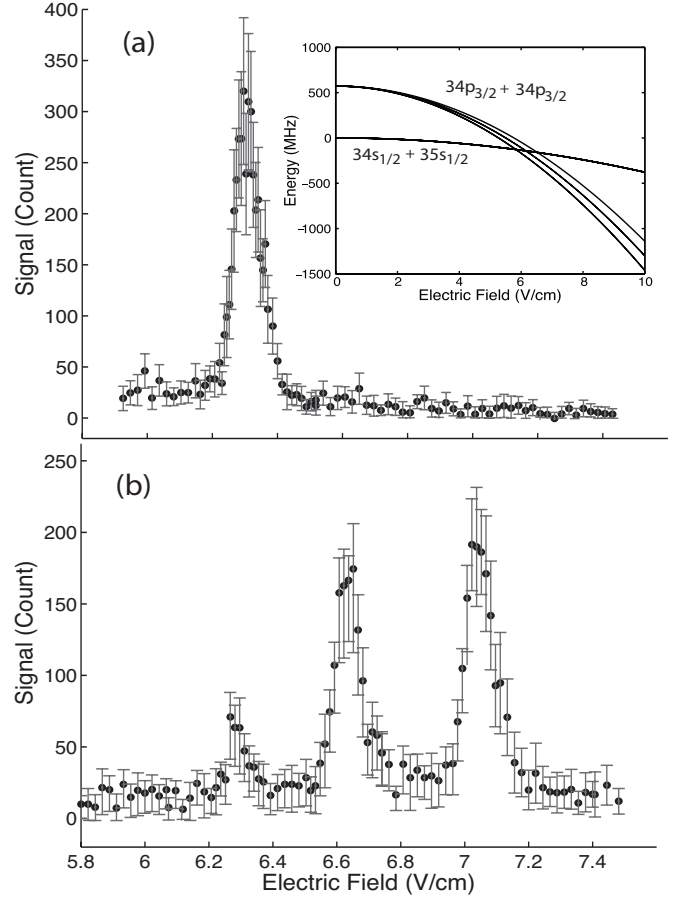

Figure 1. (a) Förster resonance for the process $34p_{3/2,|m_j|=1/2} + 34p_{3/2,|m_j|=1/2} \rightarrow 34s_{1/2} + 35s_{1/2}$. The polarization of the excitation laser is in the z direction; (b) The polarization of the excitation laser is in the x direction. Inset: Stark structures of the pair states for $34p + 34p \rightarrow 34s + 35s$ resonant energy transfer interaction.

two polarizations of the excitation laser – the number of detected $34s$ atoms after $5s_{1/2}$ atoms excited to the $34p_{3/2}$ state are allowed to interact in a static electric field for 8 μs. While the bandwidth of the p-state excitation laser is likely sufficient to also excite $34p_{1/2}$ atoms, energy level crossings do not occur for pair states with $34p_{1/2}$. We define the tuning electric field to be along the z-direction while all lasers propagate along the y-direction. In Fig.1(a), the laser was polarized parallel to z, resulting in $34p$ with only $m_j = 1/2$ and only one resonance is observed. In Fig.1(b), the laser was polarized perpendicular to z, resulting in excitation of both $m_j = 1/2$ and $m_j = 3/2$ and three resonances are observed. All three resonances are about 0.5 V/cm higher than the calculated values, but within the experimental uncertainty arising from a combination of mesh spacing and stray electric fields from the CEM.

Next, we investigated the time-dependence of the $34s$ population with and without the addition of $34d$ state
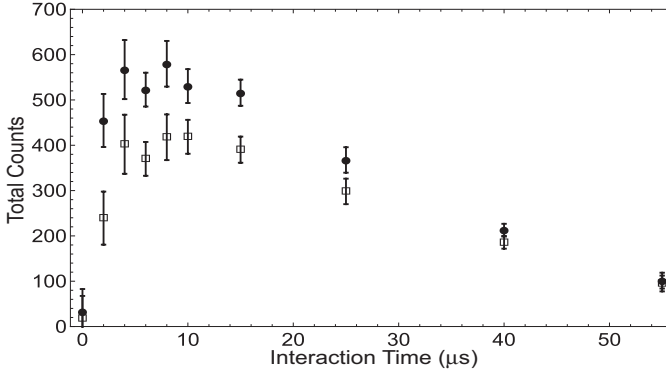
3

Figure 2. Interaction time dependence of the $34s$ state population for the resonance of $34p_{3/2,|m_j|=3/2} + 34p_{3/2,|m_j|=3/2} \rightarrow 34s_{1/2} + 35s_{1/2}$ with ($\bullet$) and without ($\square$) excitation of the $34d$ state atoms.

atoms for each of the three resonances in Fig.1b. The $34d$ excitation occurs <1 μs after the $34p$ atoms are created, although we observed that the results did not depend on whether $34p$ or $34d$ was excited first. We also confirmed that excitation of the $34d$ atoms alone produced no s-state atoms. Careful overlapping of the $34p$ and $34d$ excitation laser beams (that entered the MOT chamber from opposite directions), however, was critical. For each interaction time studied, 33 or 34 'sets' of data were collected with a set comprised of several thousand separate cycles of excitation and detection (shots) both with and without $34d$ atoms. To reduce day-to-day systematic effects arising from a change in MOT density, changes in laser power or slight changes in laser alignment, interaction times were randomly varied, but data within a set (with and without $34d$ atoms) was always taken back-to-back.

In Fig. 2, we show the time dependence of the $34s$ population for $34p_{3/2,|m_j|=3/2} + 34p_{3/2,|m_j|=3/2} \rightarrow 34s_{1/2} + 35s_{1/2}$. Each data point is an aggregate of all data sets, obtained by normalizing the counts of each individual data set for a given interaction while keeping the ratio of counts constant and then adding all of the sets together. The normalization essentially weights all sets equally and thus should be viewed as averaging over some of the systematic effects listed above that were uncontrolled in the experiment. An enhancement of $34s$ population is observed for early times. At longer times, other processes, including collisions and spontaneous emission (the $34p$ lifetime is ~30 μs) result in an observed decrease in population.

Another way to view the catalysis effect is to take the ratio of $34s$ population with and without the $34d$ atoms for each data set individually, and then average the ratios. This ensures a comparison where the experimental conditions were most similar. The result of such an analysis is given in Fig. 3 for all three Förster resonances. The error bars arise from the standard deviation of the
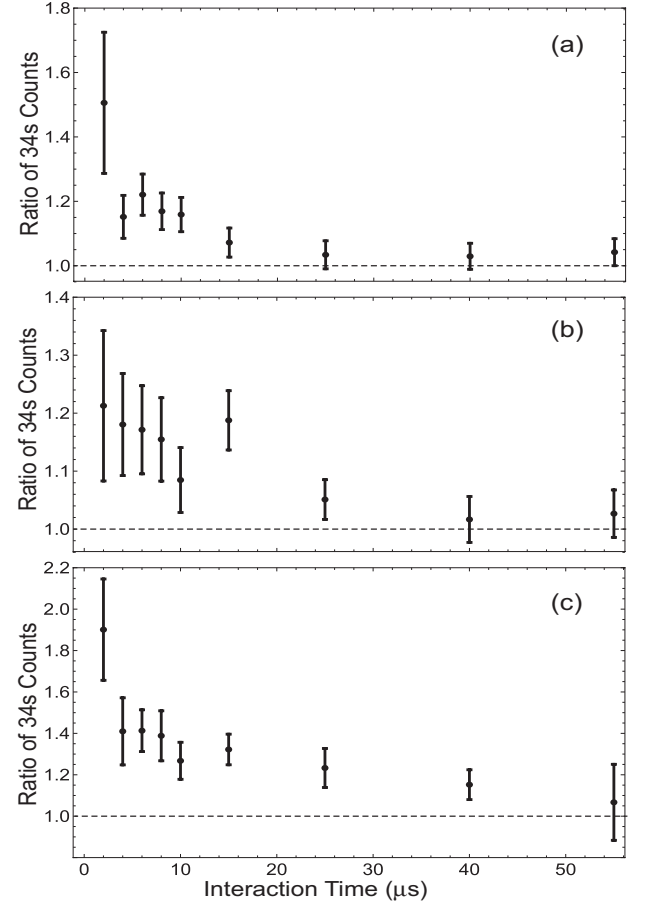

Figure 3. Ratio of the $34s$ state population vs. interaction time with and without $34d$ included in the interaction for the resonant energy transfer process: (a) $34p_{3/2,|m_j|=1/2} + 34p_{3/2,|m_j|=1/2} \rightarrow 34s_{1/2} + 35s_{1/2}$ (b) $34p_{3/2,|m_j|=3/2} + 34p_{3/2,|m_j|=1/2} \rightarrow 34s_{1/2} + 35s_{1/2}$ and (c) $34p_{3/2,|m_j|=3/2} + 34p_{3/2,|m_j|=3/2} \rightarrow 34s_{1/2} + 35s_{1/2}$. Inclusion of the $34d$ atoms alters the time evolution of the energy transfer process, especially at early times.

ratio data, which assumes a Gaussian distribution of the data points. Inspection of the actual distribution shows it to be somewhere between Gaussian and Poissonian, so the error bars are an approximation only. Clearly, the addition of $34d$ atoms enhances the $34s$ population, especially at early times. Fig. 3 (a)-(c) indicate that the measured enhancement shows some variation with initial state. This is likely in part attributable to the angular matrix elements, but further study is required to complete our understanding of the observed differences.

We have simulated the experiment by numerically solving the Schrödinger equation. Dissipation is not included in the calculation at this time. Our results point toward a mechanism for the observed enhancement. In the experiment, we translate the focus of the $34p$ excitation beam so that it fills the MOT. The $34d$ excitation beam, however, is more tightly focused to an 80 μm waist. This creates a

relatively higher density region of 34d atoms embedded within a volume of 34p atoms. The always resonant energy exchange of Eq. (2) acts to mix 34p character into the region of higher density. This produces atoms with 34p character that are closer together, allowing for more efficient transfer to the 34s and 35s states via the field tuned energy exchange of Eq. (1).

The Hamiltonian for our system in a homogeneous electric field is

$$\hat{H}_{ij} = \sum_{i \neq j} \left(\frac{\mu\nu}{R_{ij}^3}(\hat{\sigma}_{ps}^i \hat{\sigma}_{ps'}^j + \text{H.c.}) + \frac{\mu^2}{R_{ij}^3}\hat{\sigma}_{ps}^i \hat{\sigma}_{sp}^j \right.$$
$$\left. + \frac{\nu^2}{R_{ij}^3}\hat{\sigma}_{ps'}^i \hat{\sigma}_{s'p}^j + \frac{\alpha^2}{R_{ij}^3}\hat{\sigma}_{pd}^i \hat{\sigma}_{dp}^j \right)$$
$$+ \sum_i \left(E_p\hat{\sigma}_{pp}^i + E_s\hat{\sigma}_{ss}^i + E_{s'}\hat{\sigma}_{s's'}^i + E_d\hat{\sigma}_{dd}^i \right), \quad (3)$$

where μ is the $p \rightarrow s$ dipole moment, ν is the $p \rightarrow s'$ dipole moment, α is the $p \rightarrow d$ dipole moment, R_{ij} is the distance between the ith and j^{th} atoms, and $\hat{\sigma}_{xy}^i$ is an operator that changes the state of the ith atom from $|x\rangle$ to $|y\rangle$. Here s refers to the 34s and s' refers to the 35s. In an inhomogeneous field, the energies E_p, E_s, $E_{s'}$, and E_d will be a function of the atom's position. We numerically solve the Schrödinger equation on a supercomputer, assuming an initial state in which all atoms are in either the 34p or 34d state. In all of our simulation runs, we calculate the fraction of 34s atoms excited as a function of time from 0 μs to 20 μs in steps of 0.05 μs.

Our calculation includes only the 34s and 35s states, the 34$p_{3/2,|m_j|=3/2}$ state and the 34$d_{5/2,|mj|=1/2}$ state. Even with this simplification, the Hamiltonian matrix is quite large for modest numbers of atoms, so that we cannot faithfully represent the experimental geometry in simulation. Instead, we started by searching the parameter space with a model in which three 34p atoms are evenly spaced along a line. A variable number of 34d atoms, from 0 to 22, are also evenly spaced along the line. We randomly perturbed the position of each atom by a few microns and averaged over 20 instances. We ran this simulation for lengths from 50 μm to 100 μm in steps of 5 μm and for electric field gradients from 0 to 0.2 kHz/μm in steps of 0.01 kHz/μm. A gradient of 0.01 kHz/μm is equal to about 0.05 (V/cm)/cm. The $p \rightarrow s$ dipole moments increase from about 400 ea_0 at the first resonance to about 650 ea_0 at the last resonance. This is evident in Fig. 1, as the resonance peaks increase in size from left to right. However, the $p \rightarrow d$ dipole moments are no bigger than about 20 ea_0. In this model we set the $p \rightarrow s$ dipole moments to 550 ea_0 and the $p \rightarrow d$ dipole moment to 15 ea_0.

The results are shown in Fig. 4. Here, we display the ratio of 34s population with 34d atoms present to 34s population with no 34d atoms present, averaged over the full 20 μs simulation. These results show a wide range of parameters for which enhancement might be observed, suggesting that the effect is robust. However, this model also provides nearly ideal conditions; the 34p atoms are maximally spaced with 34d atoms interspersed to transport the 34p character via Eq. (2). Indeed, the largest average enhancements seen in this model, of about 2.5, are larger than the maximum enhancement seen in the experiment.

For a better comparison to the experimental results of Fig. 2 and Fig. 3, we also simulated cases in which the 34p atoms were randomly distributed in a cylindrical volume and the 34d atoms were randomly distributed within a coaxial cylindrical volume of the same length but with a smaller radius. Since the size of the basis grows so rapidly, we could not include sufficient numbers of atoms in our simulations to match the experimental conditions. In order to approximate the lower density of 34p atoms and the relatively higher density of 34d atoms, we artificially lowered the $p \rightarrow s$ dipole moments to 120 ea_0 and increased the $p \rightarrow d$ dipole moment to 50 ea_0. Our choice of simulation parameters are a compromise between matching the experiment and keeping the basis small enough to generate reasonable statistics.

The results are shown in Fig. 5 for the case a cylinder of length 80 μm with four 34p atoms in a volume with radius 9 μm and six 34d atoms in a volume with radius 5.5 μm. For this simulation, we assumed a field inhomogeneity of about 100 Hz/μm and averaged over 8000 instances. Figure 5(a) shows the fraction of atoms excited to the 34s state as a function of time. The 34s fraction increases with a timescale similar to the data in Fig. 2. Figure 5(a) compares the 34s fraction when no 34d atoms are present (dashed blue) to the 34s fraction when six 34d atoms are present (solid red). The ratio of the two signals is shown in Fig. 5(b), where a value greater than one indicates an enhancement. The inset, Fig. 5(c), displays more clearly the early time behavior where the greatest enhancement of the 34s fraction is seen.

The results of Fig. 5 are not particularly sensitive to the size and shape of the simulated volume, as long as the 34d volume is more densely populated and embedded within the 34p volume. We have tested the simulation by instead distributing the 34d atoms into the larger radius cylinder and the 34p atoms into the smaller radius cylinder. In this case, the fraction of atoms excited to the 34s state is diminished rather than enhanced, consistent with our interpretation. The simulation is quite sensitive to the field gradient; larger field gradients generate significantly more enhancement. This is because the 34d atoms are closer together and thus less affected by the field gradient so that their role in energy transport is more pronounced for larger gradients.

We have also attempted to scale the dipole moments to be closer to the experimental values. Increasing the $p \rightarrow s$ dipole moments requires increasing the size of the simulated volume so that the 34s atoms are less densely
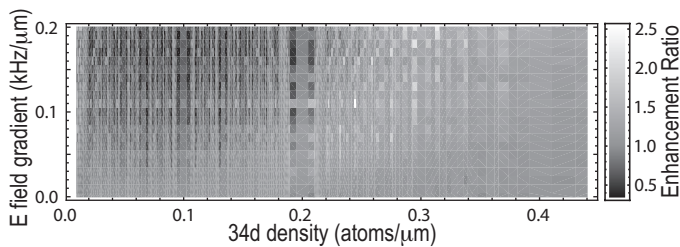
Figure 4. Simulated $34s$ signal for cases including three $34p$ atoms, a number of $34d$ atoms ranging from 0 to 22, and electric field gradients from 0 to 0.2 kHz/μm. The signal is expressed as a ratio to the case with no $34d$ atoms and averaged over 20 μs with lighter shades of gray indicating larger enhancement as shown in the legend. The atoms are evenly spaced along a line with length varied between 50 μm and 100 μm. The position of each atom is randomly perturbed by a few microns and we average over 20 instances for each unique set of parameters. The dipole moments used are similar to the experimental values. The simulation indicate a wide range of parameters for which enhancement might be visible.
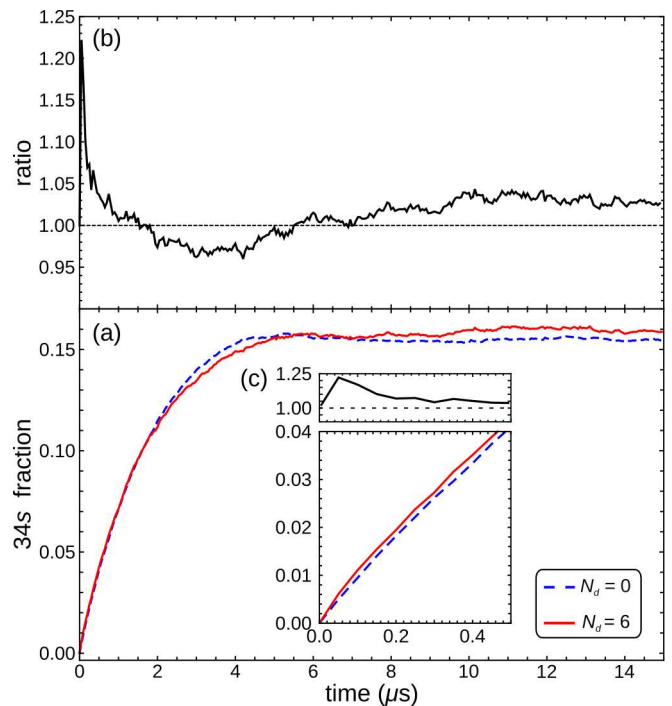

Figure 5. (color online) The $34s$ fraction at an electric field gradient of 100 Hz/μm for two coaxial 80 μm long cylinders. Four $34p$ atoms are randomly distributed over a volume with radius 9 μm and six $34d$ atoms are randomly distributed over a volume of radius 5.5 μm. The time step is 0.05 μs and we average over 8000 instances. The $p \rightarrow s$ dipole moments are set to 120 ea_0 and the $p \rightarrow d$ dipole moment is set to 50 ea_0. (a) The fraction for the case with no $34d$ atoms is shown in dashed blue and the signal with $34d$ atoms is shown in solid red. (b) The ratio of the two signals, showing enhancement that is most significant at earlier times. (c) A closer view of the early time behavior, showing where the enhancement is most pronounced.

populated. This, in turn, requires more $34d$ atoms. This procedure very quickly increases the size of the basis so that we cannot generate statistics. We have tested our simulation by increasing the $p \rightarrow s$ dipole moments from 120 ea_0 to 140 ea_0, increasing the length of the volume from 80 μm to 110 μm, and increasing the number of $34d$ atoms from 6 to 8. Encouragingly, we see results similar to those shown in Fig. 5.

In conclusion, we have investigated the Förster resonant energy transfer process of $34p + 34p \rightarrow 34s + 35s$, and observed an enhancement in $34s$ population when $34d$ state atoms are added to the mix of $34p$ atoms. Because the $34d$ atoms enhance $34s$ population but do not directly participate in the energy transfer interaction, we characterize their addition as a catalysis effect in Rydberg atom energy transfer, enabled by the addition of an interaction channel that is resonant for all electric fields: $34p + 34d \rightarrow 34d + 34p$. Although computational resources necessarily limit the initial number of atoms in our model, results are nonetheless in qualitative agreement with the experiment. Numerical simulation shows that the $34p + 34d$ channel effectively redistributes $34p$ population resulting in enhanced $p \rightarrow s$ population transfer at early times. This result could be extended by further controlling the experimental geometry, the mix of initial states and controlling electric and magnetic field gradients, potentially providing a new avenue for exploring energy transport in Rydberg systems.

[1] R. Löw, H. Weimer, J. Nipper, J. B. Balewski, B. Butscher, H. P. Büchler, and T. Pfau, J. Phys. B: At. Mol. Opt. Phys. **45**, 113001 (2012).
[2] W. R. Anderson, J. R. Veale, and T. F. Gallagher, Phys. Rev. Lett. **80**, 249 (1998).
[3] S. Wüster and J.-M. Rost, Journal of Physics B: Atomic, Molecular and Optical Physics **51**, 032001 (2018).
[4] R. A. D. S. Zanon, K. M. F. Magalhães, A. L. de Oliveira, and L. G. Marcassa, Phys. Rev. A **65**, 023405 (2002).
[5] A. L. de Oliveira, M. W. Mancini, V. S. Bagnato, and L. G. Marcassa, Phys. Rev. Lett. **90**, 143002 (2003).
[6] T. J. Carroll, K. Claringbould, A. Goodsell, M. J. Lim, and M. W. Noel, Phys. Rev. Lett. **93**, 153001 (2004).
[7] K. Afrousheh, P. Bohlouli-Zanjani, J. A. Petrus, and J. D. D. Martin, Phys. Rev. A **74**, 062712 (2006).
[8] I. I. Ryabtsev, D. B. Tretyakov, I. I. Beterov, and V. M. Entin, Phys. Rev. Lett. **104**, 073003 (2010).
[9] E. Altiere, D. P. Fahey, M. W. Noel, R. J. Smith, and T. J. Carroll, Phys. Rev. A **84**, 053431 (2011).
[10] J. Nipper, J. B. Balewski, A. T. Krupp, B. Butscher,

R. Löw, and T. Pfau, Phys. Rev. Lett. **108**, 113001 (2012).

[11] J. M. Kondo, L. F. Goncalves, J. S. Cabral, J. Tallant, and L. G. Marcassa, Phys. Rev. A **90**, 023413 (2014).

[12] T. G. Walker and M. Saffman, J. Phys. B: At. Mol. Opt. Phys. **38**, S309 (2005).

[13] T. J. Carroll, C. Daniel, L. Hoover, T. Sidie, and M. W. Noel, Phys. Rev. A **80**, 052712 (2009).

[14] K. Afrousheh, P. Bohlouli-Zanjani, J. D. Carter, A. Mugford, and J. D. D. Martin, Phys. Rev. A **73**, 063403 (2006).

[15] P. Bohlouli-Zanjani, J. A. Petrus, and J. D. D. Martin, Phys. Rev. Lett. **98**, 203005 (2007).

[16] J. A. Petrus, P. Bohlouli-Zanjani, and J. D. D. Martin, J. Phys. B: At. Mol. Opt. Phys. **41**, 245001 (2008).

[17] C. S. E. van Ditzhuijzen, A. F. Koenderink, J. V. Hernández, F. Robicheaux, L. D. Noordam, and H. B. v. L. van den Heuvell, Phys. Rev. Lett. **100**, 243201 (2008).

[18] A. Tauschinsky, C. S. E. van Ditzhuijzen, L. D. Noordam, and H. B. v. L. van den Heuvell, Phys. Rev. A **78**, 063409 (2008).

[19] V. A. Nascimento, L. L. Caliri, A. Schwettmann, J. P. Shaffer, and L. G. Marcassa, Phys. Rev. Lett. **102**, 213201 (2009).

[20] J. S. Cabral, J. M. Kondo, L. F. Goncalves, V. A. Nascimento, L. G. Marcassa, D. Booth, J. Tallant, A. Schwettmann, K. R. Overstreet, J. Sedlacek, and J. P. Shaffer, J. Phys. B: At. Mol. Opt. Phys. **44**, 184007 (2011).

[21] D. B. Tretyakov, V. M. Entin, E. A. Yakshina, I. I. Beterov, C. Andreeva, and I. I. Ryabtsev, Phys. Rev. A **90**, 041403 (2014).

[22] E. A. Yakshina, D. B. Tretyakov, I. I. Beterov, V. M. Entin, C. Andreeva, A. Cinins, A. Markovski, Z. Iftikhar, A. Ekers, and I. I. Ryabtsev, Phys. Rev. A **94**, 043417 (2016).

[23] I. Mourachko, D. Comparat, F. de Tomasi, A. Fioretti, P. Nosbaum, V. M. Akulin, and P. Pillet, Phys. Rev. Lett. **80**, 253 (1998).

[24] W. R. Anderson, M. P. Robinson, J. D. D. Martin, and T. F. Gallagher, Phys. Rev. A **65**, 063404 (2002).

[25] M. Mudrich, N. Zahzam, T. Vogt, D. Comparat, and P. Pillet, Phys. Rev. Lett. **95**, 233002 (2005).

[26] T. J. Carroll, S. Sunder, and M. W. Noel, Phys. Rev. A **73**, 032725 (2006).

[27] T. Vogt, M. Viteau, J. Zhao, A. Chotia, D. Comparat, and P. Pillet, Phys. Rev. Lett. **97**, 083003 (2006).

[28] B. Sun and F. Robicheaux, Phys. Rev. A **78**, 040701 (2008).

[29] A. Reinhard, K. C. Younge, T. C. Liebisch, B. Knuffman, P. R. Berman, and G. Raithel, Phys. Rev. Lett. **100**, 233201 (2008).

[30] A. Reinhard, T. Cubel Liebisch, K. C. Younge, P. R. Berman, and G. Raithel, Phys. Rev. Lett. **100**, 123007 (2008).

[31] A. Reinhard, K. C. Younge, and G. Raithel, Phys. Rev. A **78**, 060702 (2008).

[32] J. Han, Phys. Rev. A **82**, 052501 (2010).

[33] J. H. Gurian, P. Cheinet, P. Huillery, A. Fioretti, J. Zhao, P. L. Gould, D. Comparat, and P. Pillet, Phys. Rev. Lett. **108**, 023005 (2012).

[34] M. R. Kutteruf and R. R. Jones, Phys. Rev. Lett. **108**, 013001 (2012).

[35] D. P. Fahey, T. J. Carroll, and M. W. Noel, Phys. Rev. A **91**, 062702 (2015).

[36] J. S. Cabral, J. M. Kondo, L. F. Goncalves, L. G. Marcassa, D. Booth, J. Tallant, and J. P. Shaffer, New Journal of Physics **12**, 093023 (2010).

[37] I. Mourachko, W. Li, and T. F. Gallagher, Phys. Rev. A **70**, 031401 (2004).

[38] S. Westermann, T. Amthor, A. d. Oliveira, J. Deiglmayr, M. Reetz-Lamour, and M. Weidemüller, Eur. Phys. J. D **40**, 37 (2006).

[39] J. Schachenmayer, C. Genes, E. Tignone, and G. Pupillo, Phys. Rev. Lett. **114**, 196403 (2015).

[40] H. Bernien, S. Schwartz, A. Keesling, H. Levine, A. Omran, H. Pichler, S. Choi, A. S. Zibrov, M. Endres, M. Greiner, V. Vuletić, and M. D. Lukin, Nature **551**, 579 (2017).

[41] H. Weimer, M. Müller, I. Lesanovsky, P. Zoller, and H. P. Büchler, Nature Physics **6**, 382 (2010).

[42] I. Lesanovsky, Phys. Rev. Lett. **108**, 105301 (2012).

[43] J. P. Hague and C. MacCormick, New J. Phys. **14**, 033019 (2012).

[44] H. Schempp, G. Günter, S. Wüster, M. Weidemüller, and S. Whitlock, Phys. Rev. Lett. **115**, 093002 (2015).

[45] D. W. Schönleber, A. Eisfeld, M. Genkin, S. Whitlock, and S. Wüster, Phys. Rev. Lett. **114**, 123005 (2015).

[46] H. Yu and F. Robicheaux, Phys. Rev. A **93**, 023618 (2016).

[47] J. L. Bigelow, J. T. Paul, M. Peleg, V. L. Sanford, T. J. Carroll, and M. W. Noel, J. Phys. B: At. Mol. Opt. Phys. **49**, 164003 (2016).

[48] G. Günter, H. Schempp, M. Robert-de Saint-Vincent, V. Gavryusev, S. Helmrich, C. S. Hofmann, S. Whitlock, and M. Weidemüller, Science **342**, 954 (2013).

[49] D. P. Fahey, T. J. Carroll, and M. W. Noel, Phys. Rev. A **91**, 062702 (2015).

[50] J. D. Pritchard, *Cooperative Optical Non-linearity in a Blockaded Rydberg Ensemble*, Ph.D. thesis, Durham University (2011).